Reentrant Hexagons in Non-Boussinesq Rayleigh-Bénard Convection: Effect of Compressibility

Arun Roy and Victor Steinberg
Department of Physics of Complex Systems, The Weizmann Institute of Science, Rehovot 76100, Israel
(Received 7 February 2002; published 31 May 2002)

We present experimental studies of a new pattern sequence observed in non-Boussinesq convection in a compressible fluid near its gas-liquid critical point (CP). Besides the known hysteretic transitions among conduction state, hexagons, and rolls, another hysteretic transition from rolls to hexagons at higher values of the control parameter is found. This reentrance phenomenon is observed in a rather narrow range of about 60- to 100-μm cell heights and is attributed to large compressibility of a fluid near the CP.

DOI: 10.1103/PhysRevLett.88.244503 PACS numbers: 47.54.+r, 47.20.Bp

Competition between patterns of different symmetries in nonequilibrium nonlinear systems has been the subject of extensive studies for the last two decades. Rayleigh-Bénard convection (RBC) in a large aspect ratio cell is a paradigm, which is particularly well suited to study the problem [1]. The latter is usually treated in an Oberbeck-Boussinesq (OB) approximation, which assumes temperature and pressure independence of all physical properties of a fluid, except for thermally induced variations of density. Violation of the OB approximation results in a broken up-down symmetry, and as a consequence of this, the transition to RBC becomes of the first order instead of the second order (continuous). Moreover, the pattern, which appears above the onset, is hexagons instead of rolls as in the Boussinesq RBC case [1]. Because of these features the non-OB convection is a particularly appropriate and instructive system to study in respect to the pattern competition.

Since the seminal theoretical work of Busse [2], where bistability and hysteretic transitions between conduction and hexagons and between hexagons and rolls were predicted by using weakly nonlinear analysis, substantial experimental studies were undertaken to verify quantitatively various theoretical predictions. The OB approximation is valid for $Q^2 \ll R_c$, where R_c is the critical Rayleigh number and the parameter Q defines quantitatively the deviation from the OB approximation [2]. However, many experimental and numerical results have shown that the deviation from the OB approximation is already significant at $Q \sim 1$. The hysteretic transition between hexagons and rolls in a cylindrical cell of aspect ratio $\Gamma = 18$ (radius/height) was studied experimentally in Ref. [3], while that between the conduction state and hexagons was studied using high-resolution visualization in a large aspect ratio cell ($\Gamma = 86$) in Ref. [4]. In the latter, good quantitative agreement with the theoretical predictions of Ref. [2] was observed.

In this Letter, we report an observation of a new type of stability diagram, which exhibits reentrant hexagons above the rolls at higher values of the control parameter. These hexagons are identical with hexagons, which appeared at the convection onset. Moreover, at $Q \geq 1$ and at sufficiently high compressibility hexagons exist up to the highest values of $\mathrm{Ra}/\mathrm{Ra}_c$ reached in the experiment (about 2.2). It should be pointed out that the reentrant hexagons were observed theoretically [5] as well as experimentally in Turing patterns [6] due to the strong non-Boussinesq-like effect. However, in the latter case, hexagons, which appear below and above stripes (rolls) differ in their phase; i.e., they have either upflow or downflow in the center. Another type of coexisting upflow and downflow hexagons was observed recently in the same system but in much thicker cells, where the non-OB effect was negligible [7].

The main difference between the system under study and systems used in the previous experiments on non-OB convection is high compressibility, since we use a gas in the vicinity of its gas-liquid critical point (CP). Studies of influence of the compressibility on RBC are very scarce. While a linear stability in this case was investigated a long time ago [8], the full nonlinear problem has not been approached. Gauthier *et al.* [9] have derived an amplitude equation near the onset of steady convection in a compressible fluid. As pointed out in Ref. [9], the main difference with the classic RBC is that all orders in the nonlinearity are present. This feature can lead to a very different stability diagram and correspondingly a pattern sequence above the onset. Since the new pattern sequence reported in this Letter appears at rather moderate values of Q of the order of unity, we argue that large compressibility of a fluid near CP is responsible for the new stability diagram observed in the experiment.

We studied RBC in a high purity gas SF_6 (99.998%) in the vicinity of its CP. This fluid was chosen due to several advantages: (i) its relatively low critical temperature ($T_c = 318.73$ K) and pressure ($P_c = 37.7$ bars), (ii) well known thermodynamic and kinetic properties far away and in the vicinity of the CP, and (iii) a parametric equation of state developed recently [10]. The proximity to the CP allows us to vary the non-Boussinesq parameter at the convection onset in a wide range and to achieve extremely large aspect ratios. We varied Q by simply modifying the reduced temperature $\tau = (\bar{T} - T_c)/T_c$ from 5×10^{-4} till 10^{-2} at the critical density $\rho_c = 743.8\ \mathrm{kg/m^3}$ ($\bar{T}$ is the average temperature). We point out that for this range of variation of τ, the compressibility is varied between 0.43 and 16 bars^{-1}, which is 5–6 orders of magnitude larger than that of an ideal gas.

The convection cell bottom plate was a 0.64-cm-thick mirror-finished nickel-plated copper disk with a film heater and a thermistor used for temperature regulation. The bottom plate together with an optically flat 1.9-cm-thick sapphire window, used as the cell top, was placed in a steel pressure vessel. A Mylar spacer was used to define the sidewall and the cell height. The vessel was placed in a circulating water bath to control the temperature of the top plate. The vessel, which can withstand a pressure up to 100 bars, was first filled with SF_6 up to the critical density above CP in the T and P ranges still covered by the parametric equation of state [10]. Then the convection cell space was sealed against the rest of the gas outside the spacer by the tightening of 12 screws. Since the effect observed in our experiment depends on compressibility, the deviation of density from ρ_c can be crucially important. So the sealing procedure was conducted under simultaneous regulation of temperature to avoid such deviation.

The measurements of the cell height d and uniformity were made using an optical spectroscope with resolution better than 0.2 μm. An absolute pressure gauge with a resolution of 1 mbar and a calibrated 1000 Ω platinum resistor thermometer provided us the thermodynamic scale to define the critical parameters of the fluid and to use the parametric equation of state. The long-term temperature stability of the bath and the cell top plate was 0.7 mK rms and that of the bottom was 0.2 mK rms. The vertical diffusion time $t_v = d^2/\kappa$ was between 0.15 and 0.35 sec in the range of τ used (κ is the thermal diffusivity). In order to keep all average properties constant, $\bar{T}$ was kept constant on each step of ΔT variation by changing the top and bottom temperatures simultaneously. A high spatial resolution shadowgraph with variable magnification was used for patterns visualization and their quantitative characterization.

The experiments were performed in cells of different heights: 144, 112, 86, 72, 52, and 30 μm. However, the main quantitative results were obtained in a cell of aspect ratio $\Gamma = 116.3$ with $d = 86 \pm 0.3$ μm. Our choice of $d = 86$ μm stems from the compromise between the desire for a working range of values of τ, in which both rolls and hexagons can be stable, on the one hand, and the need for a detectable value of ΔT_c at the smallest value of τ (where ΔT_c is smallest), on the other.

Figure 1 shows a typical bifurcation plot of the pattern amplitude versus the control parameter $\epsilon = \Delta T/\Delta T_c - 1$ together with the stability range of the different patterns observed in our experiment at $\tau = 4.45 \times 10^{-3}$. The rms values of the pattern amplitude were obtained from the Fourier transforms of the background subtracted normalized images, averaged over the wave number range from 1.0 to 5.0 (d^{-1}). Near the onset the subcritical bifurcation leads to hexagons at $Q \approx 0.92$ (see the inset). In the range $0 \leq \epsilon \leq \epsilon_r$ only hexagons are stable. Then further in the range $\epsilon_r \leq \epsilon \leq \epsilon_h$ hexagons and rolls coexist. At $\epsilon \geq \epsilon_h$ only rolls are stable. Within the accuracy of the data the experimental values of the control parameter at the transitions are rather close to the calculated ones. Since we concentrate on the higher values of ϵ, we did not study the region of coexistence of hexagons and the conduction state for $\epsilon_a \leq \epsilon \leq 0$.

A surprise occurred when we further increased the value of ϵ far above ϵ_h. Then another hysteretic transition from rolls to hexagons took place. For this transition at high values of the control parameter, rolls and hexagons coexist at $\epsilon_f \leq \epsilon \leq \epsilon_j$ and at $\epsilon \geq \epsilon_j$ only hexagons are stable. Thus we found a region $\epsilon_h \leq \epsilon \leq \epsilon_f$, where only rolls

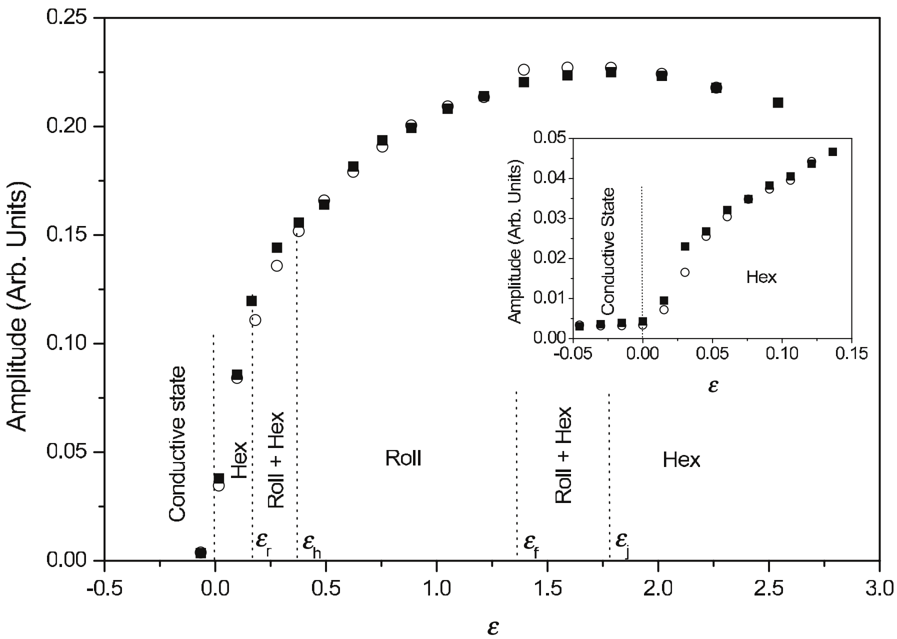

FIG. 1. Convection amplitude, obtained from the shadowgraph image, versus ϵ in a wide range of its variation at $\tau = 4.45 \times 10^{-3}$. The inset shows the region near the onset. Solid squares show the data with increasing ϵ, while open circles with decreasing one.

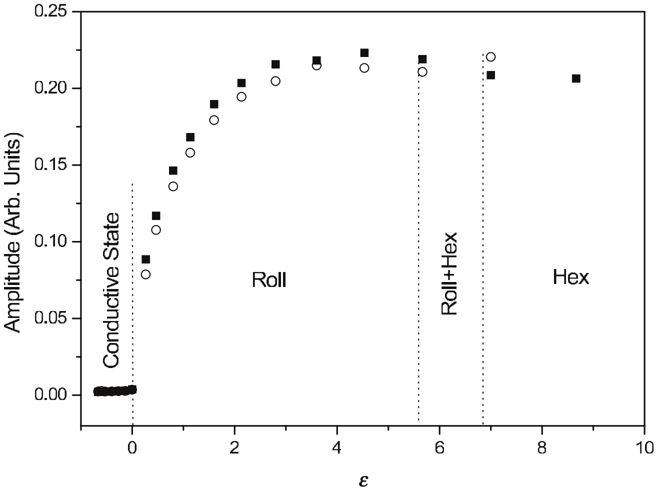

FIG. 2. Bifurcation diagram at $\tau = 2.25 \times 10^{-3}$.

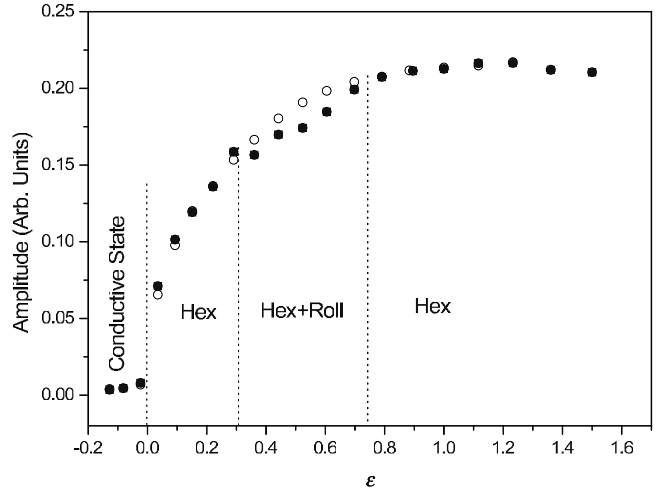

FIG. 3. Bifurcation diagram at $\tau = 5.17 \times 10^{-3}$.

are stable. Of course, due to a rather large aspect ratio, the roll structure became disordered due to the appearance of spiral-target defects which competed with rolls and led to a spiral-target defect chaos [11,13]. Such a sequence of hexagons and rolls in the non-OB RBC was never observed before and never predicted theoretically. Further, the stability range of the rolls was found to decrease with increasing values of τ. For τ higher than 5.32×10^{-3} only hexagons were found above the onset up to the highest values of ϵ reachable in the experiment.

Figures 2 and 3 show the bifurcation diagrams for another two values of $\tau = 2.25 \times 10^{-3}$ and 5.17×10^{-3}. In Fig. 2, the stability diagram did not show transition to hexagons at the convection onset due to a rather low $Q = 0.45$ at this value of τ. On the other hand, the region of pure rolls is absent in Fig. 3, because at this value of τ only region of coexistence of rolls and hexagons was found. Because the pattern amplitude was obtained in a wide range of ϵ, a nonlinearity of the shadowgraph visualization technique far away from the onset led to saturation of the pattern amplitudes at high values of ϵ. Since we used the amplitude versus ϵ plot only for qualitative illustration of the stability regions, we did not make an attempt to correct this artifact at high values of ϵ.

The stability boundaries of rolls and hexagons in the parameter space of τ and ϵ are shown in Fig. 4, where the turning point at $\tau_t \approx 5.32 \times 10^{-3}$ is clearly seen. It obviously indicates the fact that hexagons observed near the onset and far away are of the same nature and even have the same phase, i.e., reentrant hexagons. In order to reinforce this observation even further, the wave numbers of low- and high-ϵ hexagons together with the wave number of rolls, which appeared for intermediate values of ϵ, are shown in Fig. 5 for $\tau = 4.45 \times 10^{-3}$. The values of the wave numbers of both hexagons are rather close. Moreover, the wave numbers of all three types of pattern as a function of ϵ and τ show surprisingly small variations in a wide range of these parameters (see Fig. 6). It should be pointed out that in the range of τ from about 5.32×10^{-3} till 2.25×10^{-3}, a strong variation of compressibility from 0.93 to 2.6 was found. The largest value of $Q \approx 0.98$ occurred at the turning point $\tau_t \approx 5.32 \times 10^{-3}$.

A similar bifurcation diagram was also obtained for τ in the range between 1.6×10^{-3} and 3.35×10^{-3} in a cell of height 72 μm. The corresponding stability diagram is also presented in Fig. 4. We have also conducted experiments in cells of heights 144 and 112 μm and found basically the same sequence of patterns, reported in Ref. [11]. At sufficiently small Q, which occurs for these cell heights at $\tau < 10^{-2}$, first rolls and then the spiral-target chaos were found up to rather high values of ϵ. Because of the nature of our sealed cell, we were not able to reach those values of ϵ, at which coexisting hexagons show up [7]. On the other hand, in cells of heights 52 and 30 μm, hexagons were found up to the highest reachable values of ϵ for all values of τ tested.

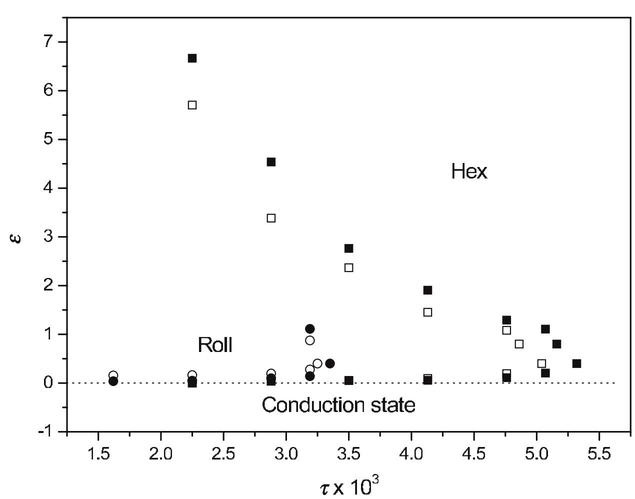

FIG. 4. Stability diagram of convection patterns for two cell heights: solid and open squares for $d = 86$ μm; solid and open circles for $d = 72$ μm. Solid symbols show the data at increasing ϵ, open symbols at decreasing one.

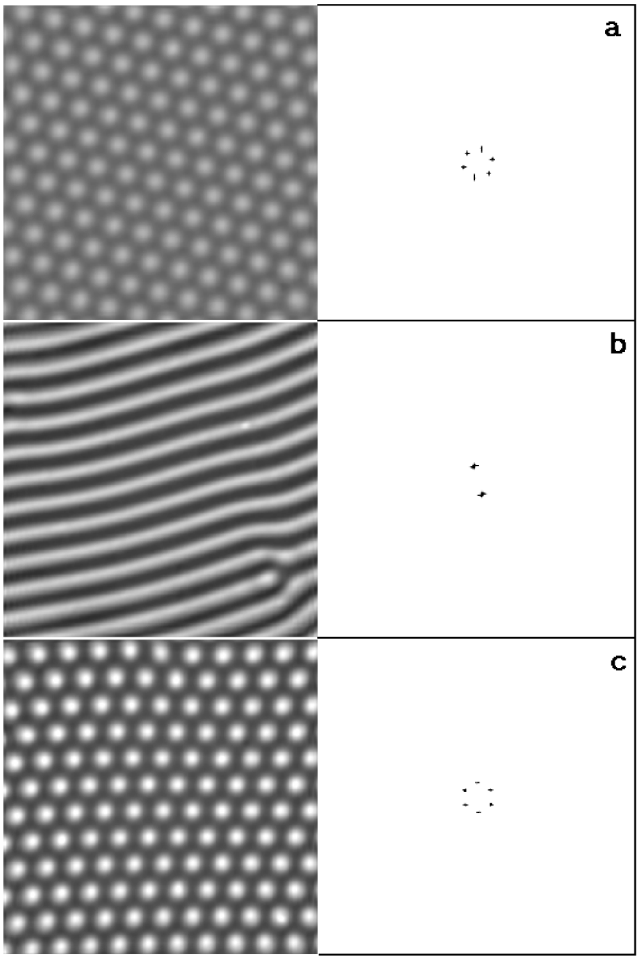

FIG. 5. Shadowgraph images and the corresponding 2D Fourier transforms of three types of patterns at $\tau = 4.45 \times 10^{-3}$ and ϵ: (a) 0.0984, (b) 0.885, and (c) 2.54.

A narrow range of the cell heights, where the new stability diagram was observed, can be explained by the following arguments. We found that at the turning point both $\epsilon_t \approx 0.4$ and $Q_t \approx 1$ were constant for two cell heights. Besides, we showed earlier that at $\rho = \rho_c$, $Q \sim \Delta T_c \tau^{-1}$, and $\Delta T_c \sim d^{-3}\tau^{\gamma+\nu}$, where $\gamma \simeq 1.24$, $\nu \simeq 0.63$ are the critical exponents [11,12]. Thus, by knowing τ_t for one cell height, one can estimate τ_t for another. This estimate gives $\tau_t = 3.2 \times 10^{-3}$ for $d = 72$ μm, where the data for $d = 86$ μm were used. This value can be compared with $\tau_t^{\exp} = 3.35 \times 10^{-3}$. Thus, using this relation one can show that in the range of τ available in our experiment, one can observe the turning point for cell heights between 60 μm ($\tau_t \approx 1.8 \times 10^{-3}$ and $\Delta T_c \approx 25$ mK) and 100 μm ($\tau_t \approx 8.4 \times 10^{-3}$ and $\Delta T_c \approx 245$ mK). Upper values of the cell height are limited by the value of compressibility sufficient to get the new instabilities, while the lower ones are limited by the experimental resolution and stability in τ and ΔT_c.

In conclusion, we present the experimental observation of a new type of reentrance phenomenon that results from large compressibility of a fluid near its CP in RBC.

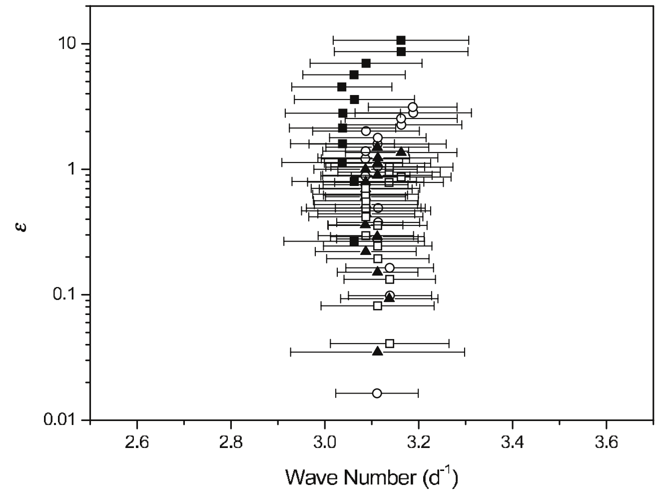

FIG. 6. Wave numbers of hexagons and rolls in a wide range of ϵ at various τ: (a) solid squares, 2.25×10^{-3}; (b) open circles, 4.45×10^{-3}; (c) solid triangles, 5.17×10^{-3}; (d) open squares, 5.51×10^{-3}. Full widths at half maximum of the wave number distributions are also shown.

This work was partially supported by the Minerva Foundation and the Minerva Center for Nonlinear Physics of Complex Systems.

[1] M. C. Cross and P. C. Hohenberg, Rev. Mod. Phys. **65**, 851 (1993).
[2] F. H. Busse, J. Fluid Mech. **30**, 625 (1967); Rep. Prog. Phys. **41**, 1929 (1978).
[3] S. Ciliberto, E. Pamploni, and C. Perez-Garcia, Phys. Rev. Lett. **61**, 1198 (1988).
[4] E. Bodenschhatz, J. R. DeBruyn, G. Ahlers, and D. S. Cannell, Phys. Rev. Lett. **67**, 3078 (1991).
[5] J. Verdasca, A. De Wit, G. Dewel, and P. Borckmans, Phys. Lett. A **168**, 194 (1992).
[6] Q. Ouyang and H. L. Swinney, Nature (London) **352**, 610 (1991).
[7] M. Assenheimer and V. Steinberg, Phys. Rev. Lett. **76**, 756 (1996).
[8] M. Gitterman and V. Steinberg, J. Appl. Math. Mech. **34**, 305 (1970).
[9] S. Gauthier, T. Desmarais, and G. Iooss, Europhys. Lett. **10**, 543 (1989).
[10] A. Abbaci and J. Sengers, Institute for Physical Sciences and Technology, University of Maryland Technical Report No. BN1111, 1990; A. Kostrowicka Wyszalkowska and J. V. Sengers, J. Chem. Phys. **111**, 1551 (1999).
[11] M. Assenheimer and V. Steinberg, Phys. Rev. Lett. **70**, 3888 (1993); Nature (London) **367**, 345 (1994). (See also [12].)
[12] Our recent detailed measurements of ΔT_c as a function of τ in the 86 μm cell were fitted by a scaling dependence $\Delta T_c = 6361\tau^{2.04}$ with the exponent close to that found in Ref. [11] (2.04 instead of 1.89), but the coefficient is rather different and much closer to the theoretically found value [8].
[13] S. W. Morris, E. Bodenschatz, D. S. Cannell, and G. Ahlers, Phys. Rev. Lett. **71**, 2026 (1993).